

Redesign Of The Analysing Magnet In The ISIS H⁻ Penning Ion Source

S. R. Lawrie, D. C. Faircloth, A. P. Letchford, M. Westall,
M. O. Whitehead, T. Wood^a and J. Pozimski^{a, b}

^a*STFC, Rutherford Appleton Laboratory, Chilton, Didcot, Oxfordshire OX14 0QX, United Kingdom*

^b*Department of Physics, Imperial College, London SW7 2AZ, United Kingdom*

Abstract. A full 3D electromagnetic finite element analysis and particle tracking study is undertaken of the ISIS Penning surface plasma H⁻ ion source. The extraction electrode, 90° analysing magnet, post-extraction acceleration gap and 700 mm of drift space have been modelled in CST Particle Studio 2008 to study the beam acceleration and transport at all points in the system. The analysing magnet is found to have a sub-optimal field index, causing beam divergence and contributing the beam loss. Different magnet pole piece geometries are modelled and the effects of space charge investigated. The best design for the analysing magnet involves a shallower intersection angle and larger separation of the pole faces. This provides radial focusing to the beam, leading to less collimation. Three new sets of magnet poles are manufactured and tested on the Ion Source Development Rig to compare with predictions.

Keywords: H⁻, Negative Ion Source, Low Energy Beam Transport, Dipole Magnet, Analysing Magnet, Weak Focusing, Plasma Electrode, Extraction Electrode

PACS: 29.95.Ni, 41.75.Cn, 41.85.Lc

APPARATUS SETUP

The ISIS H⁻ Penning ion source¹ at the Rutherford Appleton laboratory (RAL) is one of the most successful in the world, due to its long service and gradual development over the years. The continual advancement of technology in the source has led to a high average beam current of 55 mA and a pulse length of up to 1.5 ms.

A Front End Test Stand (FETS) is being constructed at RAL to demonstrate that a high power H⁻ beam can be produced for future proton accelerators with sufficient beam quality². The design criteria for the 65 keV beam produced from the FETS ion source is to have 60 mA current over a 2 ms pulse length, with horizontal and vertical normalised RMS emittances below 0.3π mm mRad. New power supplies and ancillary equipment are being constructed to meet the design specification, but the ion source will be identical to that used on ISIS, save for slight modifications needed to produce a beam with high current but low emittance. To generate the necessary modifications, experiments are performed on the Ion Source Development Rig³ (ISDR) at ISIS. This apparatus, shown in Figure 1, allows experiments to be performed on an identical copy of the ISIS source, so as not to interrupt the user schedule for ISIS neutrons.

Ion Source Development Rig

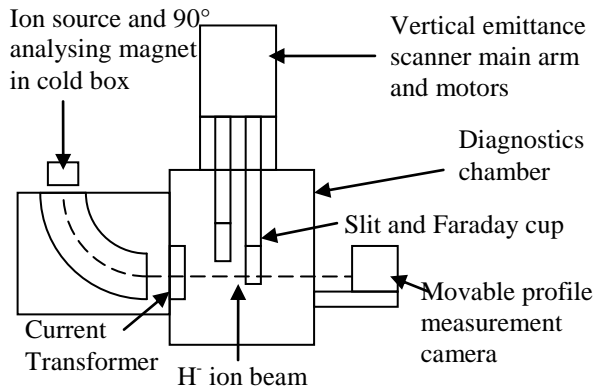


FIGURE 1. The Ion Source Development Rig. Horizontal slit-slit scanner omitted for clarity.

Finally, a pepperpot head can be mounted in front of the scintillator in order to measure the emittance and profile simultaneously.

On the ISDR, a suite of diagnostic tools are used to fully study the beam. A fast toroid is used to measure the beam current. The amount of electron stripping can be measured using a dipole magnet to separate neutrals from the H⁻ beam. The energy spread of the beam can be measured. Horizontal and vertical slit-slit scanners are used to measure the beam emittance. The beam's profile can be studied at different positions along the beam's path using a quartz scintillator and fast camera.

The ISIS Ion Source

The ISIS and ISDR H⁻ ion sources, shown in Figure 2, are of the Penning (PIG) surface plasma type. The H⁻ beam is formed from a slit-shaped plasma electrode aperture using an extraction electrode held at +17 kV. To analyse out extracted electrons, the beam then passes through a 90° sector dipole magnet. The sector magnet is housed in a cold box, used to condense excess caesium vapour and prevent it propagating downstream. After leaving the coldbox, the beam crosses the Post-Extraction Acceleration Gap (PEAG), gaining a further 18 keV of energy as it is accelerated to laboratory ground potential, resulting in a total beam energy of 35 keV. The PEAG on ISIS is presently

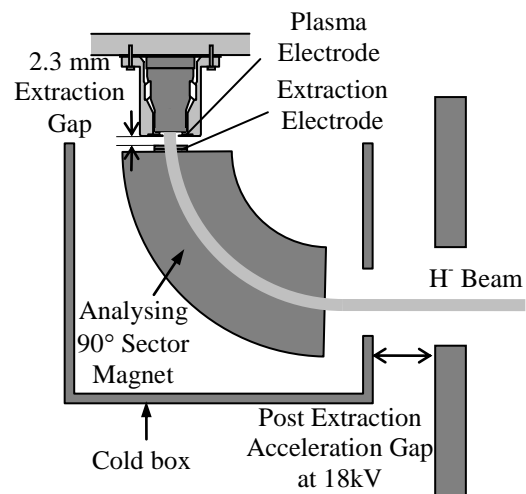


FIGURE 2. Ion source setup.

rather large at 55 mm. Its 0.327 kV mm^{-1} electric field is too low to produce an einzel lens of sufficient strength to focus the beam sufficiently, resulting in large beam losses due to collimation upon entry into the solenoid Low Energy Beam Transport (LEBT). Experiments varying the electric field strength on the ISDR by changing the PEAG have vastly improved the beam focusing.

Simulations and experiments⁴ have shown that a PEAG electric field of 9 kV mm^{-1} is optimal in terms of reducing the beam emittance. On the ISDR, therefore, a PEAG

of 2 mm, with an applied potential of 18 kV, is used to fulfil this criterion. This small gap has successfully focussed the beam both horizontally and vertically, significantly reducing the emittance, as shown in Figures 3 and 4; nevertheless the emittance is still much too large for the FETS requirements.

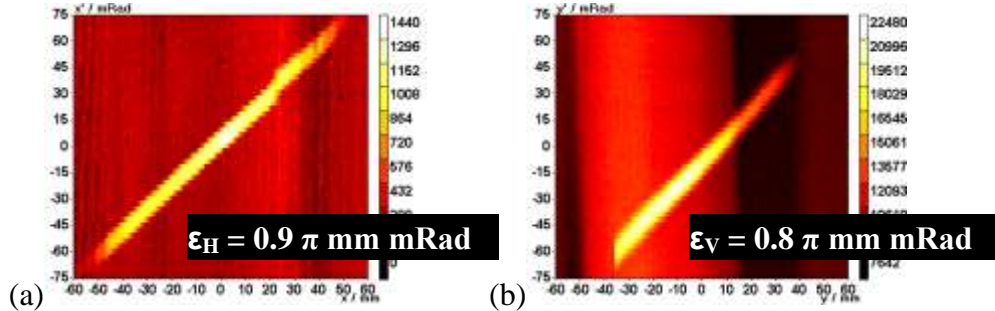


FIGURE 3. Horizontal (a) and vertical (b) emittance plots for 55 mm PEAG.

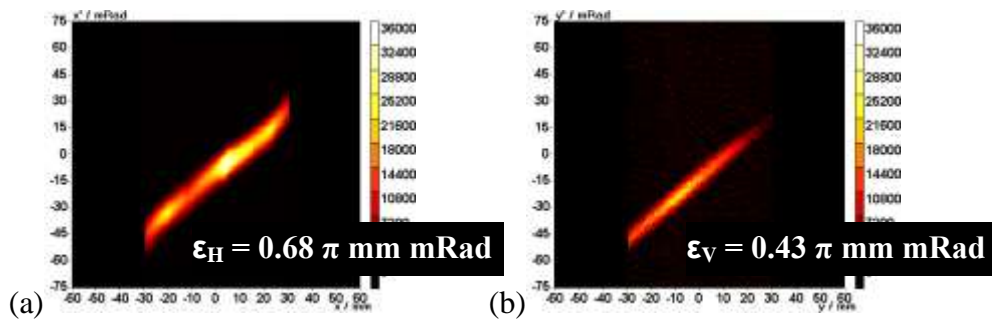


FIGURE 4. Horizontal (a) and vertical (b) emittance plots for a 2 mm PEAG. Unfortunately, the minimum scanning range in (b) was limited to -30 mm so some beam is missing, leading to a smaller emittance. If the entire beam were covered, the emittance is likely to be closer to $0.5 \pi \text{ mm mRad}$.

Beam Characteristics

Using the smaller post extraction acceleration gap of 2 mm, studies at low extraction energies showed⁵ that the beam has an asymmetrical ‘cobra-head’ shape, which is wide at the top and long and tapered at the bottom. The degree of vertical defocusing is extreme, even with an optimal PEAG electric field. To see why, a set of five plasma electrode plates were manufactured with circular extraction apertures placed at positions along the standard slit aperture. It was found that – despite being extracted from a circular aperture – each beamlet still had a distinctive ‘cobra-head’ shape⁶. The only other component in the ion source which may focus the beam is the sector magnet, so a divergent beam indicates that the sector magnet is imperfect.

WEAK FOCUSING FORCES IN THE SECTOR MAGNET

To ensure parallel beam transport around a dipole magnet, the magnetic field must be inversely proportional to the radius. Hence the magnetic field

$$B = B_e \left(\frac{R_e}{R} \right)^n \quad (1)$$

where $n = 1$ and R_e is the optimum radius at which the beam is steered around. In the ISIS ion source, $R_e = 80$ mm. For a 17 keV beam, this leads to the optimum magnetic field at R_e of $B_e = 0.235$ T. If $n \neq 1$, it can be directly calculated by rearranging (1) that

$$n = - \frac{R_e}{B_e} \left(\frac{dB}{dR} \right) \quad (2)$$

where n is the magnetic field index, and is a measure of the quadrupole component of the field inside a dipole magnet caused by the curvature of the field at the edges of the pole faces⁷. A value of the magnetic field index other than unity leads to non-parallel beam transport round a dipole magnet. This effect is Weak Focussing.

Specifically, $n < 1$ means the magnetic field is too weak at small radii and too strong at large radii, resulting in radial focussing. Conversely, $n > 1$ leads to defocusing. This being the case, it was suspected that the ISIS ion source sector magnet had a magnetic field index greater than unity, and hence was radially defocusing the beam, causing the stretched out ‘cobra-head’ shape.

An electromagnetic finite element model of the ion source was created in CST Particle Studio⁸ to study how weak focusing affected beam transport in the ion source.

Studying the Magnetic Field Index

Having solved the magnetostatic field, n was calculated using a Visual Basic macro. Plotting n as a function of radius in the dipole at the mid-plane between the pole faces, as shown in Figure 6, one see that $n_{R_e} = 1.35$. Therefore, the sector magnet does have a slightly sub-optimal geometry, causing the radial defocusing of the beam.

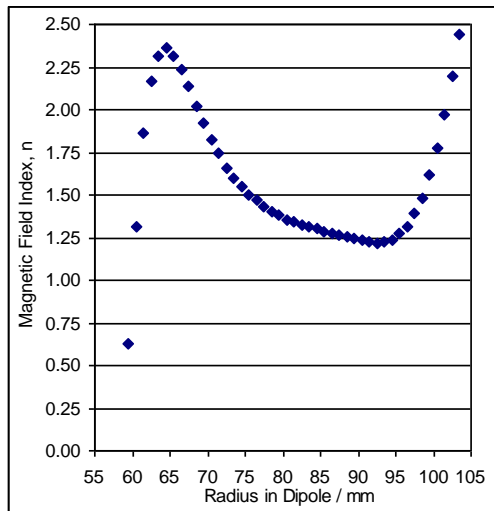


FIGURE 6. The magnetic field index of the ISIS analysing magnet.

The area where the field index is approximately constant – the “good field region” – only extends about 10 mm either side of R_e . This is due to the small 55 mm radial width of the pole pieces. 5 mm wide, 1 mm tall shims on the inner and outer radii are used in an attempt to mitigate fringe field effects but these actually make the field index worse. The obvious solution to this problem is to increase the radial width of the pole pieces. The maximum width allowable by the internal dimensions of the cold box is 74 mm. In order to vary n , either the intersection angle or the separation of the pole faces must be changed. For the ISIS poles – which have an intersection

angle of 17.76° – it was found that to achieve a field index $n = 1$, the gap between the faces would have to increase from 25 mm to 28.6 mm. In fact, $n = 1$ can be achieved for any intersection angle, providing the gap is varied. Varying the intersection angle for a fixed gap of 32 mm in Figure 7, one can see not only how n_{Re} changes, but also the shape of n in the good field region.

Note that in Figure 7 and all successive plots, the magnetic fields were calculated for pole pieces with the wider 74 mm radial width in order to maximise the good field region.

It is not only the field index at the mid-plane of the gap that is important, though. If the magnetic field, and the subsequent n , is not sufficiently uniform across the whole of the gap, this limits the size of the good field region in the transverse direction. Sampling the magnetic field at three positions away from the mid-plane in

Figure 8, the shape of n changes as the field is sampled closer the pole face. If one wants to study this effect in more detail, then the line graph in Figure 8 is insufficient. Therefore, in Figure 9 the same magnetic field is sampled at a higher resolution across the gap, with the value of n represented as colours in a contour plot.

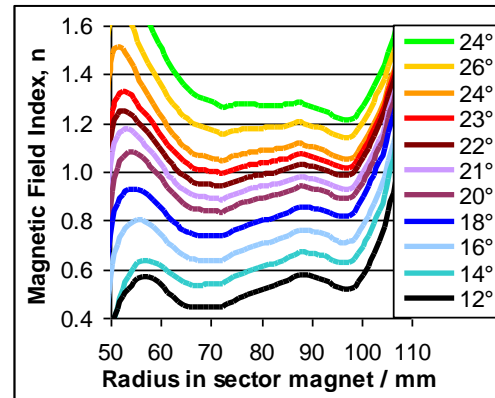


FIGURE 7. How n changes when varying the dipole face intersection angle.

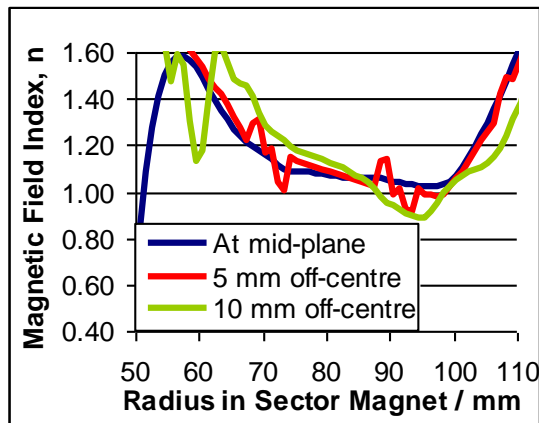


FIGURE 8. Variation of n at positions away from the centre of the gap

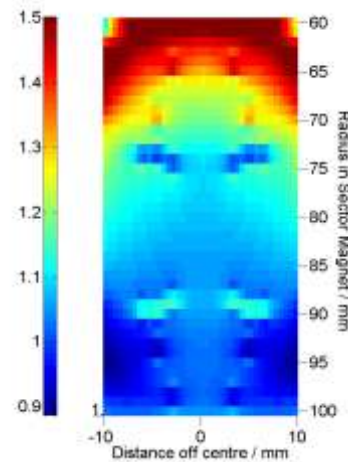


FIGURE 9. Contour plot of the magnetic field index as a function of position in the gap

With this new technique to study how the pole piece geometry affects the magnetic field index, it is now simple to accurately design new pole pieces for any desired n .

PARTICLE TRACKING THROUGH THE ISIS ION SOURCE

To test the accuracy of the ion source CAD model and the solved electro- and magnetostatic fields in CST, particle tracking of the H^- beam was performed. A drift

space of 700 mm was included in the model in order to compare the beam profiles at a position level with the slit-slit emittance scanners.

Previous attempts to simulate the shape of the beam have been unsuccessful; giving a rectangular profile rather than the distinctive ‘cobra-head’ seen on the ISDR. Indeed, performing particle tracking in CST produces this result when no space charge is present in the model. However there are reasons why space charge should be included:

1. Space charge compensating particles exist in drift sections of an accelerator, due to residual gas interactions, but not in accelerating regions. Therefore space charge must be taken into account in the extraction gap and PEAG.
2. At the standard operating conditions of +17 kV extraction and 35 keV total beam energy, the beam profile is round. However lowering the extraction energy reveals the cobra-head structure, indicating that the beam is collimating at higher energies as it passes through the PEAG.
3. Simulations with no space charge show a small beam totally dissimilar in shape to the real beam and which does not come close to collimating.

Experiments including space charge in the entire beam path caused the beam to be enormously divergent due to its low energy and large areas of drift relative to the size of the acceleration gaps. This confirmed that space charge should only be considered in the extraction and post-extraction acceleration gaps. When this arrangement was simulated, the resulting beam had the profile shown in Figure 10; to be compared with the real measured beam in Figure 11. The impressive agreement between the two indicates both that the electromagnetic and particle tracking solvers are accurate and that space charge is necessary in order to correctly simulate the beam.

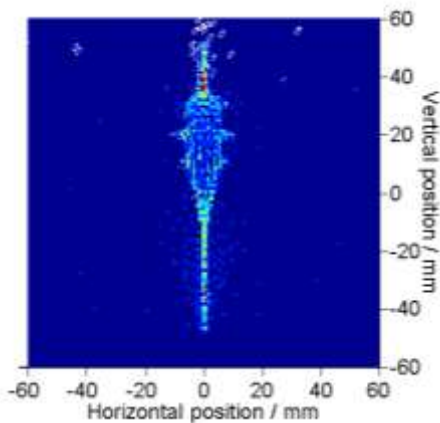


FIGURE 10. Particle tracking solution for the ISIS ion source sector magnet geometry.

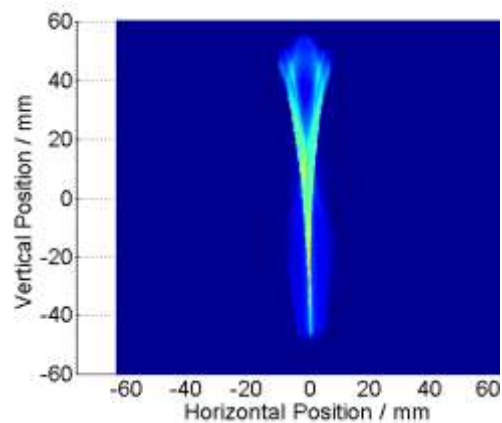


FIGURE 11. Beam profile from the ISIS ion source using a quartz scintillator and CCD.

With the standard ISIS H^- beam successfully re-created for the first time, improvements could be made to the sector magnet with confidence that the simulated beams from new pole pieces would be seen in the lab.

Design of the New Sector Magnet Pole Pieces

In order to improve the beam transport through the ion source, the good field region of the sector magnet was enlarged by widening the pole pieces radially to 74 mm. To see how this widening affects the beam, a set of poles with the same intersection angle, centre gap and shims as the old poles was created. Next, a set of poles with a field index $n = 1$ was designed, with the shims modified in order to enlarge the good field region still further, so as to keep $n = 1$ across the entire gap. Finally, in order to add radial focussing to the beam, pole pieces were made which have $n = 0.75$. The shims on the outer radius are shaped so as to increase the local magnetic field and hence guide errant particles back in to R_e . The contour plots of n for these new poles are shown in Figure 12 along with the plot for the old ISIS poles.

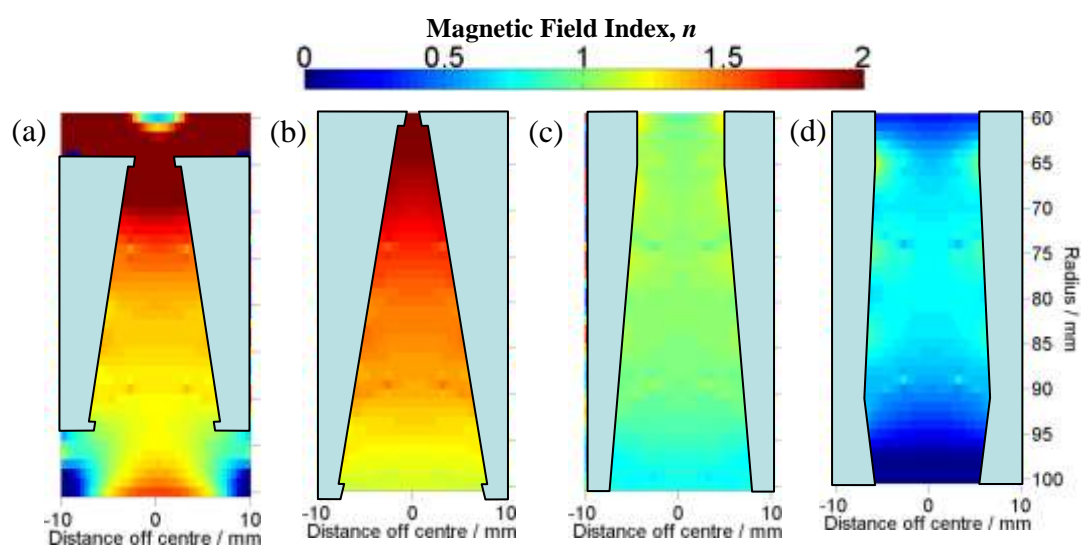


FIGURE 12. Contour plots of n for (a) the standard ISIS pole pieces; (b) ISIS pole pieces with wider radial extent; (c) $n = 1$ poles; (d) $n = 0.75$ poles with enlarged shims at the outer radius. Note the enlarged good field region in (b) compared to that in (a). Representations of the pole piece are overlaid on the contour plots for comparison, but are not to scale.

One further modification to the pole pieces was the cut-off from 90° of the sector magnet closest to the cold box exit. A cut-off is used in order to prematurely stop the magnetic field; otherwise the fringe field extent is such as to over-steer the beam vertically. Previous modelling work⁹ has shown that the beam emerges parallel and on axis from the cold box when the cut-off is 3 mm and a tube of high permeability “maximag” steel is inserted to the cold box exit hole to remove fringe fields. However these models were performed with very little or no drift space after the cold box hole.

The present simulation has 700 mm of drift space, and it is clear that the beam does indeed emerge from the cold box on axis, but thereafter veers upward due to cumulative influence of the tiny fringe field remaining a substantial distance downstream. To remove this effect, the cut-off has been increased to 14 mm, which allows the residual field to fine tune the beam’s vertical alignment. In this manner, the beam is correctly aligned to enter the first solenoid of the LEBT parallel and on axis.

With these modifications implemented to the pole pieces, particle tracking was performed. The predicted beam profiles from the new poles are shown in Figure 13.

Explanation For The Predicted Beam Shapes

It can be seen that for smaller n , the beam becomes smaller in the radial (vertical) direction as predicted, but spreads in the axial (horizontal) direction.

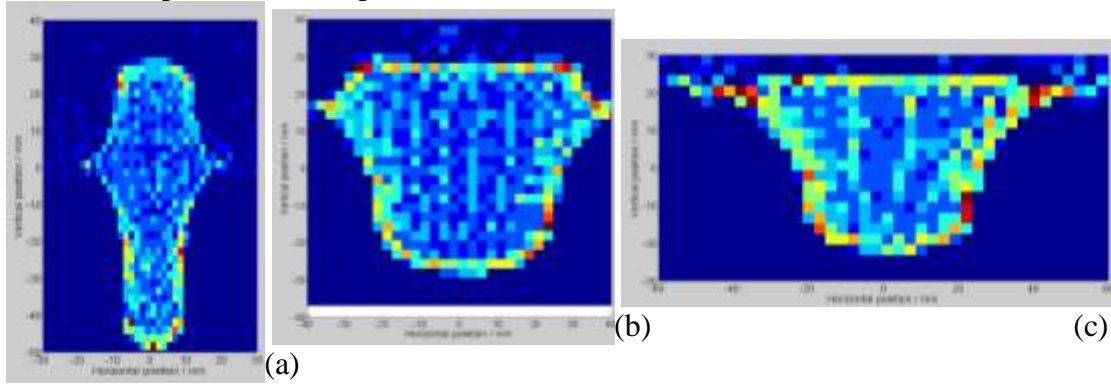


FIGURE 13. Predicted beam profiles for (a) Widened ISIS, (b) $n = 1$ and (c) $n = 0.75$ pole pieces. The $n = 1$ poles create the roundest beam. Note that the long tails above and below the beam core seen in Figures 10 and 11 are now absent due to the wider radial extent of the new pole pieces.

It may be tempting to attribute the asymmetrical focusing to the beam's space charge redistributing itself, but space charge is fully compensated in the majority of the model. The reason in fact lies with the magnetic field index once more. The sector magnet can be thought of as a 90° portion of a cyclotron accelerator, where weak focussing forces are very important in the design. Particles in these accelerators undergo betatron oscillations around the equilibrium radius – both in the radial direction and the axial direction⁷. The frequencies of these oscillations, ω_R and ω_z respectively, with respect to the desired cyclotron orbit frequency, ω_c are

$$\omega_R = \omega_c \sqrt{1 - n} \quad (3)$$

$$\omega_z = \omega_c \sqrt{n} \quad (4)$$

Radial orbital stability in a cyclotron only occurs for $0 < n < 1$, therefore the imaginary value obtained in Eq. 3 for the radially divergent beam from the $n = 1.35$ ISIS ion source is to be expected.

Using Eq. 4 it is clear that for $n = 1$ pole pieces in a cyclotron, a particle beam undergoes one axial oscillation for every orbit around the cyclotron. Therefore for the ion source sector magnet, which is one quarter of an orbit, the beam would spread to its maximum axial size. For the $n = 1.35$ pole pieces, the beam has gone past its maximum axial extent and started converging again, whereas for the $n = 0.75$ pole pieces the beam has not quite reached its maximum spread. These facts explain why the $n = 1$ beam profile in Figure 13 has the largest horizontal (axial) width. [IS THIS SHOWN IN FIGURE 13?]

EXPERIMENTAL RESULTS USING THE NEW POLE PIECES

A comprehensive study of the beam profile, emittance and current for each set of pole pieces was performed. The results for a 17 keV extracted beam are shown in Figures 14 and 15 for two of the three sets of sector magnet pole pieces. When compared to the old set of poles in Figure 4, the vertical emittance is reduced due to the increased radial width, with a further reduction when $n = 1$.

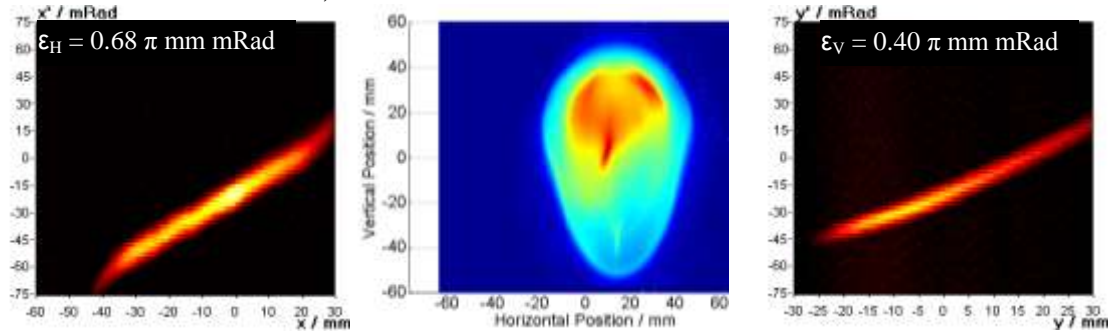


FIGURE 14. Beam emittance and profile from widened ISIS pole pieces with 17kV extraction energy.

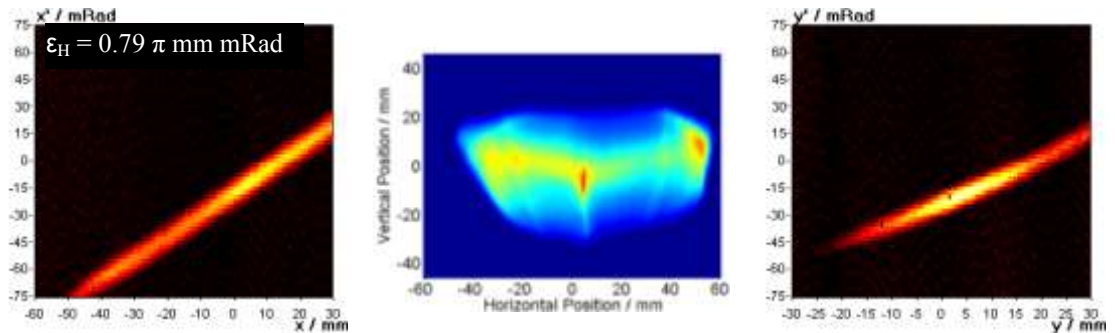


FIGURE 15. Beam emittance and profile from $n = 1.0$ pole pieces with 17kV extraction energy.

Unfortunately, power supply failures delayed testing of the $n = 0.75$ set of pole pieces. However the substantial agreement between the beam profiles measured in Figures 14 and 15 to those calculated in Figure 13 means the beam from the $n = 0.75$ poles is likely to have the shape predicted.

The horizontal emittance is largest for the $n = 1.0$ pole pieces, in agreement with Eq. 4. However, because the extraction electrodes also apply horizontal divergence to the beam, different extraction geometries were implemented in order to reduce the horizontal emittance. The electrode configurations used were: 0.6 x 10 mm slit aperture plasma electrode, with either open-ended or closed 2.1 mm separated extraction jaws (this is the standard ISIS extraction geometry); a 0.8 x 10 mm slit aperture, used to extract greater beam current; small circular apertures positioned along the slit; and extraction geometry with the Pierce angle¹⁰.

As can be seen in Figure 16, for the widened ISIS pole pieces the emittance continues to increase roughly linearly with extraction energy. However, in Figure 17, the beam from the $n = 1$ pole pieces reaches a limit in its horizontal emittance. For both sets of pole pieces, the horizontal emittance is reduced by approximately 15% when using the Pierce extraction geometry. Therefore, the minimum normalised RMS

emittance values currently achievable for a 17 keV extracted beam accelerated to a total energy of 35 keV are $\epsilon_H = 0.59$ and $\epsilon_V = 0.33 \pi$ mm mRad. Emittance values and errors were calculated using the SCUBEE algorithm¹¹.

The maximum beam current achieved at all extraction energies was when using the 0.8 mm wide plasma electrode aperture slit, up to a maximum of 76 mA at 20 keV. Nevertheless, over 60 mA was achievable with all extraction geometries.

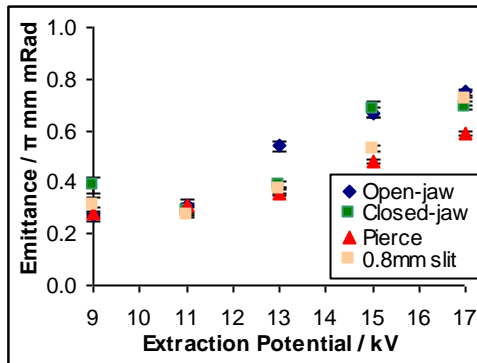


FIGURE 16. Horizontal emittance for widened ISIS pole pieces.

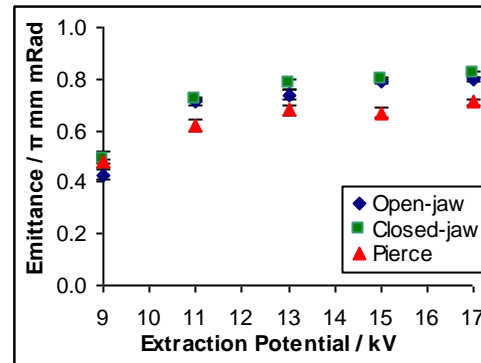


FIGURE 17. Horizontal emittance for $n = 1$ pole pieces.

CONCLUSIONS

Modelling the ISIS ion source with space charge and drift space included in the simulation has successfully produced the ‘cobra-head’ beam profile which collimates at high extraction energies. Modifying the radial width, intersection angle and separation of the sector magnet pole pieces allows weak focusing forces to alter the shape of the beam and prevent collimation.

Experiments using the new pole pieces have shown the beam profile to be very similar to that predicted. By modifying the magnetic field index, the beam divergence has been reduced enough in the vertical direction to meet the FETS criterion for emittance. The horizontal emittance is still too large; however using the Pierce extraction electrode geometry, this has been somewhat reduced. The current requirements for FETS can be achieved using any extraction or sector magnet setup; but the 0.8 mm wide aperture slit produces the greatest beam current, which may become important for longer pulse lengths.

The thorough investigation of the effects of both the extraction and sector magnet geometries has led to great progress in the understanding of beam transport through the ion source. This knowledge will help ensure that the H⁻ beam from the ISIS ion source has the correct properties for use in FETS and other future projects.

REFERENCES

1. R. Sidlow et. al., EPAC '96, THP084L.
2. D. C. Faircloth, “Commissioning of the Front End Test Stand High Performance H⁻ Ion Source at RAL”, these proceedings.
3. J. W. G. Thomason et. al., EPAC '02, THPRI012.

4. D. C. Faircloth et. al., EPAC '08, MOPC142.
5. D. C. Faircloth et. al., Rev. Sci. Instrum. 79 (2008), 02B717.
6. D. C. Faircloth et. al., EPAC '08, MPOC143.
7. J. J. Livingood, "Principles of Cyclic Particle Accelerators", Van Nostrand, Princeton, NJ (1961).
8. CST Studio Suite 2008, www.cst.com
9. D. C. Faircloth et. al., Rev. Sci. Instrum, 75 (2004), 1735.
10. J. R. Pierce, "Theory and Design of Electron Beams", 2nd ed., Van Nostrand, Princeton, NJ (1954).
11. M. P. Stockli et. al., Rev. Sci. Instrum. 75 (2004), 1646.